EUROPEAN ORGANIZATION FOR NUCLEAR RESEARCH

CERN–PPE/92–209
December 4, 1992

Determination of Quark Electroweak Couplings from Direct Photon Production in Hadronic Z Decays

L3 Collaboration

Abstract

We report on a comparison of isolated hard photon production in hadronic Z decays with the predictions of a next-to-leading order matrix-element calculation. We constrain the quark electroweak couplings to the Z boson with a simultaneous fit to three direct photon distributions, and combine this result with an independent constraint from our measurement of the total hadronic width of the Z, obtaining $c_{\mathrm{u}} = 0.92 \pm 0.22$ and $c_{\mathrm{d}} = 1.63 \pm 0.15$ where $c_{\mathrm{u,d}} = 4\,(\overline{g}_{\mathrm{V}}^2 + \overline{g}_{\mathrm{A}}^2)_{\mathrm{u,d}}$. Our results are consistent with Standard Model predictions.

(Submitted to *Physics Letters B*)

Introduction

Isolated hard photons (direct photons) produced in hadronic Z decays are mainly associated with radiation from the primary quark-antiquark pair. These events provide information about the electroweak couplings of quarks[1], and serve as probes of the short-distance structure of QCD. LEP is particularly well-suited for direct photon studies[2–5] because of a high event rate and suppressed initial-state radiation.

The decay of a Z boson into a quark-antiquark pair can be described by two effective electroweak coupling constants, $c_{\rm u,d} = 4\,(\overline{g}_{\rm V}^2 + \overline{g}_{\rm A}^2)_{\rm u,d}$, where the subscripts u and d denote charge $+2/3$ (u-type) and charge $-1/3$ (d-type) quarks respectively. These couplings contribute only to the overall rate of a process involving the decay of a Z into quarks. We consider here two such processes: the inclusive decay of a Z into hadrons, and the decay of a Z into hadrons together with photon radiation from the primary quark-antiquark pair. The linear combination of couplings that appears in the expression for the total hadronic decay width of the Z is already well-constrained experimentally [6–10]. New measurements of isolated hard photons in hadronic events offer the possibility to determine a different linear constraint that, when combined with the total width measurement, allows us to infer the individual values of the u- and d-type quark electroweak couplings.

In order to relate the observed production of isolated hard photons to the electroweak coupling factor that appears in the cross-section, we must first calculate the factor in the cross-section that does not depend on the couplings. This factor can be expressed as a phase-space integral of appropriate matrix elements, where experimental cuts are included as phase-space constraints, and was first calculated by Kramer and Lampe[11]. More recent theoretical work[12–14] has focussed on the treatment of essentially non-perturbative contributions to the matrix-element calculation that were not considered in ref. [11].

We report here on a comparison of our direct photon data, already presented in ref. [4], with the predictions of a QCD matrix-element calculation at $\mathcal{O}(\alpha\,\alpha_{\rm s})$. We determine a linear constraint on the quark electroweak couplings with a simultaneous fit to three direct photon distributions and, combining this fit with our measurement of the the total hadronic decay width of the Z [8], obtain the individual values of the u- and d-type quark electroweak couplings.

The L3 Detector

The L3 detector[15] consists of a central tracking chamber, a high resolution electromagnetic calorimeter composed of bismuth germanium oxide crystals, a ring of scintillation counters, a uranium and brass hadron calorimeter with proportional wire chamber readout, and an accurate muon chamber system. These detectors are installed in a 12 m diameter, 16 m long magnet, which provides a uniform field of 0.5 T along the beam direction.

The material in front of the electromagnetic calorimeter amounts to less than 10% of a radiation length. The energy resolution for electrons and photons is better than 2% for energies above 1.5 GeV. The angular resolution for electromagnetic clusters with energies above 5 GeV is better than 2 mrad.

Data Analysis

The data analysis relevant to this paper has been previously described in ref. [4]. We briefly summarize its main features.

Hadronic events with direct photons are chosen by first selecting hadronic events as described in ref. [8], and further requiring that the center-of-mass energy be in the range 91.0 – 91.5 GeV, in order to reduce the contribution from initial-state photons and interference between initial and final state radiation. This procedure yields 323 674 events collected during 1990 and 1991.

In each of these events, photon candidates are selected from the barrel region of the electromagnetic calorimeter, covering the polar angles 45° – 135°, where the contribution from initial-state photons is minimal. Photon candidates are defined as clusters in the electromagnetic calorimeter that have an energy greater than 5 GeV, that are not associated with a charged track, and that are isolated by at least 15° from other electromagnetic-calorimeter clusters of energy greater than 500 MeV. Finally, jets are reconstructed from the hadronic part of the event (excluding the photon candidate) using the JADE algorithm[16] with the parameter $y_{cut} = 0.05$. We require that photon candidates be isolated by more than 20° from the axis of each reconstructed jet.

We find 3202 events with isolated hard photon candidates. Monte Carlo studies indicate that in addition to final-state photons radiated from quarks, this sample includes neutral hadrons occurring either as single isolated particles or in tight groups of particles that decay into adjacent photons, as well as a smaller fraction of initial-state photons. We directly identify and reject the low-energy neutral hadron background in our sample by its characteristic pattern of energy deposition in the electromagnetic calorimeter. We subtract the remaining high-energy neutral hadron and initial-state photon background statistically from our final distributions by inferring their contributions from a large sample of simulated Monte Carlo events.

In order to facilitate comparisons with theoretical models, the data in ref. [4] have been corrected for detector effects: a correction factor for each bin is calculated as the ratio of the number of Monte Carlo events selected with energy and jet-isolation cuts in an ideal detector, to the number of events selected with all cuts in a simulated L3 detector. The data in fig. 3 of ref. [4] are reproduced in fig. 1, and give the corrected distributions of the final-state photon energy, the angle between photons and the nearest jet, and the transverse energy of photons with respect to the event thrust axis.

Theoretical Predictions

In the Standard Model, the interaction of a fermion, f, with a Z boson proceeds via vector and axial neutral currents, with effective coupling constants $\overline{g}_{\mathrm{V}}$ and $\overline{g}_{\mathrm{A}}$. We formulate our results in terms of the combined effective coupling

$$c_{\mathrm{f}} \equiv 4 \left(\overline{g}_{\mathrm{V}}^2 + \overline{g}_{\mathrm{A}}^2\right)_{\mathrm{f}} \ . \tag{1}$$

In the improved Born approximation c_{f} is related to the charge of the fermion, Q_{f}, via[17]

$$c_{\mathrm{f}} = \rho_{\mathrm{eff}} \left[1 + \left(1 - 4\ |Q_{\mathrm{f}}|\ \sin^2\overline{\theta}_{\mathrm{W}}\right)^2\right] \ , \tag{2}$$

where $\overline{\theta}_W$ is the effective weak mixing angle and $\rho_{\mathrm{eff}} \sim 1$ includes electroweak corrections. The decay of a Z boson into quark-antiquark pairs is then described by two combined coupling constants: one for u-type quarks (c_{u}) with $Q_{\mathrm{u}} = +2/3$, and one for d-type quarks (c_{d}) with $Q_{\mathrm{d}} = -1/3$.

The total hadronic decay width of the Z is given in the improved Born approximation by[18]

$$\Gamma\left(\mathrm{Z} \rightarrow \mathrm{q}\overline{\mathrm{q}}\right) = \frac{N_c m_{\mathrm{Z}}^3 G_\mu}{24\pi\sqrt{2}} \left[1 + \frac{\alpha_{\mathrm{s}}}{\pi} + 1.4\left(\frac{\alpha_{\mathrm{s}}}{\pi}\right)^2\right] \left(2\, c_{\mathrm{u}} + 3\, c_{\mathrm{d}}\right) , \tag{3}$$

where $N_c = 3$ denotes the number of colours, m_{Z} is the mass of the Z boson, and G_μ is the muon decay constant. The middle factor gives QCD corrections calculated to second order in the next-to-leading order strong coupling constant, α_{s}. The last factor describes the electroweak coupling of the Z boson to quarks: u and c quarks contribute 2 c_{u}; d, s, and b quarks contribute 3 c_{d}. Corrections to eq. (3) due to quark masses and higher-order diagrams involving extra photons and gluons are negligible.

A distribution derived from the decay of a Z into a quark-antiquark pair, together with a photon radiated from one of the quarks, has the general form

$$\mathrm{d}\sigma(\mathrm{Z} \rightarrow \mathrm{q}\overline{\mathrm{q}}\gamma) = \mathcal{F} \times \mathcal{N} , \tag{4}$$

with

$$\mathcal{N} = 2\, c_{\mathrm{u}} \cdot Q_{\mathrm{u}}{}^2 + 3\, c_{\mathrm{d}} \cdot Q_{\mathrm{d}}{}^2 , \tag{5}$$

in the approximation that all quarks are massless. Compared with eq. (3), the electroweak factor, $\mathcal{N}$, contains additional weightings of Q^2, reflecting the fact that the photon couples to fermions in proportion to their charge squared. The matrix element factor, $\mathcal{F}$, describes the effect of experimental cuts for selecting isolated hard photons, as well as the effects of QCD corrections. Matrix elements for one-, two- and three-jet production in combination with a photon are related to the matrix elements for two-, three- and four-jet processes without photons, as described in ref. [11]. Integrating these matrix elements gives an expression of the form

$$\mathcal{F} = \frac{\alpha}{2\pi}\left(f_0 + \frac{\alpha_{\mathrm{s}}}{2\pi} f_1 + \mathcal{O}(\alpha_{\mathrm{s}})^2\right) + \mathcal{O}(\alpha)^2 , \tag{6}$$

where f_0, f_1 denote the leading order ($\mathcal{O}(\alpha)$) and next-to-leading order ($\mathcal{O}(\alpha\,\alpha_{\mathrm{s}})$) contributions.

An important aspect of the calculation is the treatment of infrared divergences in the matrix elements. These are associated with configurations with a soft gluon or photon ('soft divergence') and configurations with a gluon or photon collinear with a quark ('collinear divergence'). The divergences due to soft and collinear gluons cancel with virtual gluon contributions for cross-sections defined in terms of suitably resolved jets, rather than quarks and gluons[19]. We define two partons to be resolved when their combined invariant mass exceeds some minimum value, $\sqrt{ys}$, where $\sqrt{s}$ is the center-of-mass energy of the event.

Infrared divergences due to soft photons are avoided by selecting hard photons; however, divergences due to photons collinear with soft quarks can not be avoided with any reasonable photon isolation criteria[12–14]. Thus, this collinear photon singularity is an unavoidable feature of the calculation, reflecting our incomplete knowledge of non-perturbative contributions[12]. In order to make finite predictions from perturbation theory, a second parameter, $\theta_{\mathrm{q}\gamma}$, is added to the calculation[12–14] in addition to the jet resolution, y, and the experimental cuts. The parameter $\theta_{\mathrm{q}\gamma}$ appears in the calculation as a phase-space cut on the minimum angle between a quark and a photon, and plays the role of a factorization scale between perturbative and non-perturbative contributions.

The parameter α_{s} appearing in eq. (6) is a measure of the effective quark-gluon coupling in events with an isolated hard photon, including leading-order gluon corrections. This parameter is difficult to relate to experimental determinations of the strong coupling constant which are measured in different processes and take account of higher-order gluon corrections. For the present calculation, α_s should be estimated from a comparison of data with a leading-order QCD calculation. In the following, we use the notation $\alpha_s^{(1)}$ to distinguish the parameter appearing in eq. (6) from the next-to-leading order strong coupling constant.

Several computer programs have recently been described[12–14, 20] for calculating f_0 and f_1 of eq. (6). These programs all agree on the essential features of the matrix elements, and offer similar options for defining the phase space allowed in a calculation. We use the program described in ref. [14] which is particularly suited to our analysis.

Results

In this section we first compare our previous measurement of the total isolated hard photon rate with the prediction of a matrix-element calculation, and then describe a more detailed comparison using three distributions, from which we obtain a constraint on the quark electroweak couplings. Finally we combine our measurement with our previous measurement of the total hadronic decay width of the Z, obtaining the individual values of the u- and d-type quark electroweak couplings, and the leading-order strong coupling constant.

In our earlier paper[4], we measured the fraction of hadronic events with photons isolated by more than 20° from jets and with energy greater than 5 GeV to be

$$\mathrm{BR}(\mathrm{Z} \to \mathrm{hadrons} + \gamma)/\mathrm{BR}(\mathrm{Z} \to \mathrm{hadrons}) = (5.2 \pm 0.3 \pm 0.4) \times 10^{-3} \ ,$$

where the first error is statistical and the second error is systematic. The calculation of this quantity, assuming massless quarks and the Standard Model couplings, is considered in detail in ref. [14] and yields

$$\mathrm{BR}(\mathrm{Z} \to \mathrm{hadrons} + \gamma)/\mathrm{BR}(\mathrm{Z} \to \mathrm{hadrons}) = (5.8 \pm 0.4) \times 10^{-3} \ ,$$

where the theoretical uncertainty is estimated by varying the collinear photon cut, $\theta_{\mathrm{q}\gamma}$, between 10° and 20°, and the leading-order strong coupling constant, $\alpha_s^{(1)}$, between 0.1 and 0.2. Thus we find agreement between our data and the calculation of ref. [14] for the overall rate of isolated hard photons.

In order to make a more detailed test of the agreement between the matrix-element calculation and our data, we compare the distributions in fig. 1 with the theoretical predictions for these distributions. This approach allows us to reduce the uncertainty in the theoretical prediction by constraining $\alpha_s^{(1)}$ directly from our data.

We determine the theoretical predictions by first calculating the coefficients f_0 and f_1 of eq. (6) for each bin of each distribution. These coefficients depend on the experimental cuts on photon energy and isolation from jets, as well as the phase-space cuts y and $\theta_{\mathrm{q}\gamma}$[14]. We choose the value $y = 5 \times 10^{-5}$ for the parton resolution parameter, as a compromise between minimizing recombination artefacts, and numerical efficiency. We choose three values of the collinear-photon cut, $\theta_{\mathrm{q}\gamma} = 10°$, 15°, and 20°, to cover a range that reasonably reflects the theoretical uncertainty due to uncalculable non-perturbative effects and respects technical limitations of the calculation. For a given value of the leading-order strong coupling, $\alpha_s^{(1)}$, and the electroweak couplings, c_{u} and c_{d}, we calculate three theoretical predictions (corresponding to three values of $\theta_{\mathrm{q}\gamma}$) for each bin via eq. (5) and eq. (6) with $\alpha = 1/137$. Since the theoretical predictions are determined numerically, they have an associated numerical uncertainty which is typically

$< 1\%$. At leading order, differences between predictions with different values of $\theta_{q\gamma}$ are small ($< 1\%$ of the total rate) and only occur for photons with energy > 40 GeV that are isolated by $\sim 180^\circ$ from jets; at next-to-leading order, differences are larger ($< 10\%$ of the total rate) and most pronounced for low-energy photons (5–10 GeV) that are close to jets (20°–30°).

For each value of $\theta_{q\gamma}$ we determine both the leading-order strong coupling, $\alpha_s^{(1)}$, and the electroweak factor, $\mathcal{N}$, with a simultaneous chi-square fit to the three corrected data distributions in fig. 1. The fit parameters are almost independent of each other: the normalization of the data determines the electroweak factor and the shape of the data determines the strong coupling. There is a weak correlation between the parameters due to a small dependence of the theoretical normalization on $\alpha_s^{(1)}$. The fit uses the program MINUIT[21], and takes account of both statistical and systematic errors in the data, as well as numerical uncertainties in the theoretical prediction. Systematic errors in the corrected data are mostly due to background subtraction; studies indicate that these errors primarily reflect an uncertainty in the normalization of the background to be subtracted. In the fit, we assume that systematic errors on the corrected data are correlated entirely through normalization. This procedure tends to overestimate the error on the electroweak factor and underestimate the error on the leading-order strong coupling, and is thus conservative from the point of view of determining the electroweak couplings. Fit results are summarized in table 1. Fig. 1 shows comparisons of the fitted matrix-element predictions with $\theta_{q\gamma} = 10^\circ$ and 20°, to our corrected data.

$\theta_{q\gamma}$	$\mathcal{N}$	$\alpha_s^{(1)}$	χ^2/DF
10°	1.28 ± 0.12	0.167 ± 0.023	24.4/25
15°	1.32 ± 0.13	0.171 ± 0.025	25.2/25
20°	1.37 ± 0.13	0.163 ± 0.030	31.9/25

Table 1: Results of simultaneous chi-square fits to three corrected data distributions, using three values of the collinear-photon cutoff parameter, $\theta_{q\gamma} = 10^\circ$, 15°, and 20°. Fit parameters are the electroweak factor, $\mathcal{N}$, and the leading-order strong coupling constant, $\alpha_s^{(1)}$.

In order to assess the effects of hadronization on the theoretical prediction, we have calculated the leading-order coefficients using the central value $\theta_{q\gamma} = 15^\circ$, both with and without fragmentation of partons. We fragment partons with the program JETSET 7.3[22] using parameters tuned to give a good overall description of hadronic events[23]. The effect of fragmentation on the leading-order prediction is small compared with the effect of the next-to-leading order correction. We consider the difference between the fitted parameters with and without fragmentation as the hadronization uncertainty.

Our matrix-element calculation assumes that all quarks are massless. We have studied the effects of a 5 GeV b-quark with the Monte-Carlo programs JETSET[22] and HERWIG[24], and with an $\mathcal{O}(\alpha)$ matrix-element calculation including mass-terms. These indicate that we can account for a massive b-quark in the theoretical prediction by using the massless-quark matrix-element factor combined with a modified electroweak factor

$$\mathcal{N} = 2\, c_\mathrm{u} \cdot {Q_\mathrm{u}}^2 \; + \; (2+\epsilon)\, c_\mathrm{d} \cdot {Q_\mathrm{d}}^2 \,, \qquad (7)$$

with $\epsilon = 0.8 \pm 0.1$. The uncertainty in ϵ reflects the range in values predicted by different models.

For a combined result, we average the fitted values for different values of $\theta_{q\gamma}$. We estimate the uncertainty in the combined result due to the choice of collinear-photon cut as half the difference between the extreme fitted values. For the constraint on the electroweak couplings, we make a second estimate as half the difference between the extreme values that result from fits in which $\alpha_s^{(1)}$ is fixed at 0.167. The two uncertainty estimates for $\mathcal{N}$ are 0.04 and 0.07, and we conservatively choose the larger, coming from the second estimate. Our combined results are

$$\begin{aligned}\mathcal{N} &= 1.32 \pm 0.13(\text{exp}) \pm 0.01(\text{hadr}) \pm 0.07(\text{col.cut}) \\ \alpha_s^{(1)} &= 0.167 \pm 0.030(\text{exp}) \pm 0.022(\text{hadr}) \pm 0.004(\text{col.cut})\ ,\end{aligned}$$

where the experimental error is dominated by the uncertainty in the normalization of the data. The linear constraint on c_u and c_d from this combined result is shown in fig. 2 as a broad band.

For a cross-check on the value of the leading-order strong coupling constant, it is useful to compare with an independent estimate. We use our measured fraction of hadronic Z decays with a three-jet structure[25] together with a parameterization of the leading-order QCD prediction for this quantity[18], and find $\alpha_s^{(1)} = 0.19$ which is in agreement with the value obtained above.

In ref. [8] we performed a simultaneous fit to all of our measured cross-section data, to determine the Z mass, the total Z width, and the partial widths for leptonic and hadronic decays. Assuming lepton universality, we obtained $m_Z = 91.181 \pm 0.022$ GeV and $\Gamma(\text{Z} \rightarrow \text{hadrons}) = 1742 \pm 19$ MeV. Including our measurements of the forward-backward asymmetry for leptonic Z decays, we also obtained $\sin^2\overline{\theta}_W = 0.227 \pm 0.007$, and $\rho_{\text{eff}} = 1.000 \pm 0.011$, within the framework of the Standard Model.

Evaluating eq. (3) with our measured values of m_Z and $\Gamma(\text{Z} \rightarrow \text{hadrons})$, we calculate

$$2\,c_u + 3\,c_d = 6.720 \pm 0.076\ ,$$

using the value $\alpha_s = 0.125 \pm 0.009$ from ref. [26] for calculating the QCD corrections, and taking account of parameter correlations. Fig. 2 shows this linear constraint on c_u and c_d as a narrow band. By combining this limit from the total hadronic decay width of the Z with the previous limit from fits to our direct photon data, we obtain

$$c_u = 0.92 \pm 0.22 \quad , \quad c_d = 1.63 \pm 0.15\ ,$$

where b-quark mass effects are included and change the results by $< 7\%$. The error is dominated by the uncertainty in the overall normalization of our direct photon data. We calculate the quark electroweak couplings within the framework of the Standard Model by evaluating eq. (2). We obtain

$$c_u = 1.156 \pm 0.014 \quad , \quad c_d = 1.486 \pm 0.015\ ,$$

taking account of parameter correlations. Thus, the values obtained above are consistent with Standard Model predictions. Fig. 2 shows the quark couplings calculated with eq. (2) as a circle. Our results agree with previous measurements reported in refs. [3, 5].

Conclusions

We have compared our data on isolated hard photons produced in hadronic Z decays with the predictions of a matrix element calculation. We find good agreement between our data and a next-to-leading order calculation in which the quark electroweak couplings are not constrained to their Standard Model values, from which we obtain a linear constraint on the couplings. We derive a second linear constraint on the couplings from our measurement of the Z hadronic decay width. By combining these two limits we determine the individual values of the u- and d-type quark electroweak couplings. Our findings are consistent with Standard Model predictions.

Acknowledgements

We express our gratitude to the CERN accelerator divisions for the excellent performance of the LEP machine. We also acknowledge the effort of all engineers and technicians who have participated in the construction and maintenance of this experiment.

The L3 Collaboration:

O.Adriani,[14] M.Aguilar-Benitez,[23] S.Ahlen,[9] J.Alcaraz,[15] A.Aloisio,[26] G.Alverson,[10] M.G.Alviggi,[26] G.Ambrosi,[31] Q.An,[16] H.Anderhub,[45] A.L.Anderson,[13] V.P.Andreev,[35] T.Angelov,[13] L.Antonov,[39] D.Antreasyan,[7] P.Arce,[23] A.Arefiev,[25] A.Atamanchuk,[35] T.Azemoon,[3] T.Aziz,[8,1] P.V.K.S.Baba,[16] P.Bagnaia,[34] J.A.Bakken,[33] L.Baksay,[41] R.C.Ball,[3] S.Banerjee,[8] J.Bao,[5] R.Barillère,[15] L.Barone,[34] A.Baschirotto,[24] R.Battiston,[31] A.Bay,[17] F.Becattini,[14] U.Becker,[13,45] F.Behner,[45] J.Behrens,[45] S.Beingessner,[4] Gy.L.Bencze,[11] J.Berdugo,[23] P.Berges,[13] B.Bertucci,[31] B.L.Betev,[39,45] M.Biasini,[31] A.Biland,[45] G.M.Bilei[31] R.Bizzarri,[34] J.J.Blaising,[4] G.J.Bobbink,[15,2] M.Bocciolini,[14] R.Bock,[1] A.Böhm,[1] B.Borgia,[34] M.Bosetti,[24] D.Bourilkov,[28] M.Bourquin,[17] D.Boutigny,[4] B.Bouwens,[2] E.Brambilla,[26] J.G.Branson,[36] I.C.Brock,[32] M.Brooks,[21] C.Buisson,[22] A.Bujak,[42] J.D.Burger,[13] W.J.Burger,[17] J.Busenitz,[41] X.D.Cai,[16] M.Capell,[20] M.Caria,[31] G.Carlino,[26] F.Carminati,[14] A.M.Cartacci,[14] R.Castello,[24] M.Cerrada,[23] F.Cesaroni,[34] Y.H.Chang,[13] U.K.Chaturvedi,[16] M.Chemarin,[22] A.Chen,[47] C.Chen,[6] G.M.Chen,[6] H.F.Chen,[18] H.S.Chen,[6] J.Chen,[13] M.Chen,[13] M.L.Chen,[3] W.Y.Chen,[16] G.Chiefari,[26] C.Y.Chien,[5] M.Chmeissani,[3] M.T.Choi,[40] S.Chung,[13] C.Civinini,[14] I.Clare,[13] R.Clare,[13] T.E.Coan,[21] H.O.Cohn,[29] G.Coignet,[4] N.Colino,[15] A.Contin,[7] F.Crijns,[28] X.T.Cui,[16] X.Y.Cui,[16] T.S.Dai,[13] R.D'Alessandro,[14] R.de Asmundis,[26] A.Degré,[4] K.Deiters,[13] E.Dénes,[11] P.Denes,[33] F.DeNotaristefani,[34] M.Dhina,[45] D.DiBitonto,[41] M.Diemoz,[34] H.R.Dimitrov,[39] C.Dionisi,[34,15] M.T.Dova,[16] E.Drago,[26] T.Driever,[28] D.Duchesneau,[17] P.Duinker,[2] I.Duran,[37] S.Easo,[31] H.El Mamouni,[22] A.Engler,[32] F.J.Eppling,[13] F.C.Erné,[2] P.Extermann,[17] R.Fabbretti,[43] M.Fabre,[43] S.Falciano,[34] S.J.Fan,[38] O.Fackler,[20] J.Fay,[22] M.Felcini,[15] T.Ferguson,[32] D.Fernandez,[23] G.Fernandez,[23] F.Ferroni,[34] H.Fesefeldt,[1] E.Fiandrini,[31] J.Field,[17] F.Filthaut,[28] G.Finocchiaro,[34] P.H.Fisher,[5] G.Forconi,[17] T.Foreman,[2] K.Freudenreich,[45] W.Friebel,[44] M.Fukushima,[13] M.Gailloud,[19] Yu.Galaktionov,[25,13] E.Gallo,[14] S.N.Ganguli,[15,8] P.Garcia-Abia,[23] S.S.Gau,[47] D.Gele,[22] S.Gentile,[34,15] S.Goldfarb,[10] Z.F.Gong,[18] E.Gonzalez,[23] P.Göttlicher,[1] A.Gougas,[5] D.Goujon,[17] G.Gratta,[30] C.Grinnell,[13] M.Gruenewald,[30] C.Gu,[16] M.Guanziroli,[16] J.K.Guo,[38] V.K.Gupta,[33] A.Gurtu,[8] H.R.Gustafson,[3] L.J.Gutay,[42] K.Hangarter,[1] A.Hasan,[16] D.Hauschildt,[2] C.F.He,[38] T.Hebbeker,[1] M.Hebert,[36] U.Herten,[1] A.Hervé,[15] K.Hilgers,[1] H.Hofer,[45] H.Hoorani,[17] G.Hu,[16] G.Q.Hu,[38] B.Ille,[22] M.M.Ilyas,[16] V.Innocente,[15] H.Janssen,[15] S. Jezequel,[4] B.N.Jin,[6] L.W.Jones,[3] A.Kasser,[19] R.A.Khan,[16] Yu.Kamyshkov,[29] P.Kapinos,[35,44] J.S.Kapustinsky,[21] Y.Karyotakis,[15] M.Kaur,[16] S.Khokhar,[16] M.N.Kienzle-Focacci,[17] J.K.Kim,[40] S.C.Kim,[40] Y.G.Kim,[40] W.W.Kinnison,[21] D.Kirkby,[30] S.Kirsch,[44] W.Kittel,[28] A.Klimentov,[13,25] A.C.König,[28] E.Koffeman,[2] O.Kornadt,[1] V.Koutsenko,[13,25] A.Koulbardis,[35] R.W.Kraemer,[32] T.Kramer,[13] V.R.Krastev,[39,31] W.Krenz,[1] A.Krivshich,[35] H.Kuijten,[28] K.S.Kumar,[12] A.Kunin,[12,25] G.Landi,[14] D.Lanske,[1] S.Lanzano,[26] P.Lebrun,[22] P.Lecomte,[45] P.Lecoq,[15] P.Le Coultre,[45] D.M.Lee,[21] I.Leedom,[10] J.M.Le Goff,[15] R.Leiste,[44] M.Lenti,[14] E.Leonardi,[34] J.Lettry,[45] X.Leytens,[2] C.Li,[18,16] H.T.Li,[6] P.J.Li,[38] X.G.Li,[6] J.Y.Liao,[38] W.T.Lin,[47] Z.Y.Lin,[18] F.L.Linde,[15] B.Lindemann,[1] D.Linnhofer,[45] L.Lista,[26] Y.Liu,[16] W.Lohmann,[44,15] E.Longo,[34] Y.S.Lu,[6] J.M.Lubbers,[15] K.Lübelsmeyer,[1] C.Luci,[34] D.Luckey,[7,13] L.Ludovici,[34] L.Luminari,[34] W.Lustermann,[44] J.M.Ma,[6] W.G.Ma,[18] M.MacDermott,[45] P.K.Malhotra,[8]† R.Malik,[16] A.Malinin,[4,25] C.Maña,[23] D.N.Mao,[3] Y.F.Mao,[6] M.Maolinbay,[45] P.Marchesini,[45] F.Marion,[4] A.Marin,[9] J.P.Martin,[22] L.Martinez-Laso,[23] F.Marzano,[34] G.G.G.Massaro,[2] T.Matsuda,[13] K.Mazumdar,[8] P.McBride,[12] T.McMahon,[42] D.McNally,[45] M.Merk,[28] L.Merola,[26] M.Meschini,[14] W.J.Metzger,[28] Y.Mi,[19] G.B.Mills,[21] Y.Mir,[16] G.Mirabelli,[34] J.Mnich,[1] M.Möller,[1] B.Monteleoni,[14] R.Morand,[4] S.Morganti,[34] N.E.Moulai,[16] R.Mount,[30] S.Müller,[1] A.Nadtochy,[35] E.Nagy,[11] M.Napolitano,[26] F.Nessi-Tedaldi,[45] H.Newman,[30] C.Neyer,[45] M.A.Niaz,[16] A.Nippe,[1] H.Nowak,[44] G.Organtini,[34] D.Pandoulas,[1] S.Paoletti,[14] P.Paolucci,[26] G.Passaleva,[14,31] S.Patricelli,[26] T.Paul,[5] M.Pauluzzi,[31] F.Pauss,[45] Y.J.Pei,[1] S.Pensotti,[24] D.Perret-Gallix,[4] J.Perrier,[17] A.Pevsner,[5] D.Piccolo,[26] M.Pieri,[15] P.A.Piroué,[33] F.Plasil,[29] V.Plyaskin,[25] M.Pohl,[45] V.Pojidaev,[25,14] N.Produit,[17] J.M.Qian,[3] K.N.Qureshi,[16] R.Raghavan,[8] G.Rahal-Callot,[45] P.G.Rancoita,[24] M.Rattaggi,[24] G.Raven,[2] P.Razis,[27] K.Read,[29] D.Ren,[45] Z.Ren,[16] M.Rescigno,[34] S.Reucroft,[10] A.Ricker,[1] S.Riemann,[44] W.Riemers,[42] K.Riles,[3] O.Rind,[3] H.A.Rizvi,[16] F.J.Rodriguez,[23] B.P.Roe,[3] M.Röhner,[1] S.Röhner,[1] L.Romero,[23] J.Rose,[1] S.Rosier-Lees,[4] R.Rosmalen,[28] Ph.Rosselet,[19] A.Rubbia,[13] J.A.Rubio,[15] H.Rykaczewski,[45] M.Sachwitz,[44] J.Salicio,[15] J.M.Salicio,[23] G.S.Sanders,[21] A.Santocchia,[31] M.S.Sarakinos,[13] G.Sartorelli,[7,16] M.Sassowsky,[1] G.Sauvage,[4] V.Schegelsky,[35] D.Schmitz,[1] P.Schmitz,[1] M.Schneegans,[4] N.Scholz,[45] H.Schopper,[46] D.J.Schotanus,[28] H.J.Schreiber,[44] R.Schulte,[1] S.Schulte,[1] K.Schultze,[1] J.Schwenke,[1] G.Schwering,[1] C.Sciacca,[26] I.Scott,[12] R.Sehgal,[16] P.G.Seiler,[43] J.C.Sens,[15,2] L.Servoli,[31] I.Sheer,[36] D.Z.Shen,[38] S.Shevchenko,[30] X.R.Shi,[30] S.Shotkin,[13] J.Shukla,[32] E.Shumilov,[25] V.Shoutko,[25] E.Soderstrom,[33] D.Son,[40] A.Sopczak,[36] C.Spartiotis,[5] T.Spickermann,[1] P.Spillantini,[14] R.Starosta,[1] M.Steuer,[7,13] D.P.Stickland,[33] F.Sticozzi,[13] H.Stone,[17] K.Strauch,[12] B.C.Stringfellow,[42] K.Sudhakar,[8] G.Sultanov,[16] R.L.Sumner,[33] L.Z.Sun,[18,16] H.Suter,[45] R.B.Sutton,[32] J.D.Swain,[16] A.A.Syed,[16] X.W.Tang,[6] L.Taylor,[10] G.Terzi,[24] C.Timmermans,[28] Samuel C.C.Ting,[13] S.M.Ting,[13] M.Tonutti,[1] S.C.Tonwar,[8] J.Tóth,[11] A.Tsaregorodtsev,[35] G.Tsipolitis,[32] C.Tully,[30] K.L.Tung,[6] J.Ulbricht,[45] L.Urbán,[11] U.Uwer,[1] E.Valente,[34] R.T.Van de Walle,[28] I.Vetlitsky,[25] G.Viertel,[45] P.Vikas,[16] U.Vikas,[16] M.Vivargent,[4] H.Vogel,[32] H.Vogt,[44] I.Vorobiev,[25] A.A.Vorobyov,[35] L.Vuilleumier,[19] M.Wadhwa,[16] W.Wallraff,[1] C.R.Wang,[18] G.H.Wang,[32] J.H.Wang,[6] X.L.Wang,[18] Y.F.Wang,[13] Z.M.Wang,[16,18] A.Weber,[1] J.Weber,[45] R.Weill,[19] T.J.Wenaus,[20] J.Wenninger,[17] M.White,[13] C.Willmott,[23] F.Wittgenstein,[15] D.Wright,[33] R.J.Wu,[6] S.X.Wu,[16] Y.G.Wu,[6] B.Wysłouch,[13] Y.Y.Xie,[38] Y.D.Xu,[6] Z.Z.Xu,[18] Z.L.Xue,[38] D.S.Yan,[38] X.J.Yan,[13] B.Z.Yang,[18] C.G.Yang,[6] G.Yang,[16] K.S.Yang,[6] Q.Y.Yang,[6] Z.Q.Yang,[38] C.H.Ye,[16] J.B.Ye,[18] Q.Ye,[16] S.C.Yeh,[47] Z.W.Yin,[38] J.M.You,[16] N.Yunus,[16] M.Yzerman,[2] C.Zaccardelli,[30] P.Zemp,[45] M.Zeng,[16] Y.Zeng,[1] D.H.Zhang,[2] Z.P.Zhang,[18,16] B.Zhou,[9] J.F.Zhou,[1] R.Y.Zhu,[30] H.L.Zhuang,[6] A.Zichichi,[7,15,16] B.C.C.van der Zwaan.[2]

1 I. Physikalisches Institut, RWTH, W-5100 Aachen, FRG[§]
III. Physikalisches Institut, RWTH, W-5100 Aachen, FRG[§]
2 National Institute for High Energy Physics, NIKHEF, NL-1009 DB Amsterdam, The Netherlands
3 University of Michigan, Ann Arbor, MI 48109, USA
4 Laboratoire d'Annecy-le-Vieux de Physique des Particules, LAPP,IN2P3-CNRS, BP 110, F-74941 Annecy-le-Vieux CEDEX, France
5 Johns Hopkins University, Baltimore, MD 21218, USA
6 Institute of High Energy Physics, IHEP, Beijing, China
7 INFN-Sezione di Bologna, I-40126 Bologna, Italy
8 Tata Institute of Fundamental Research, Bombay 400 005, India
9 Boston University, Boston, MA 02215, USA
10 Northeastern University, Boston, MA 02115, USA
11 Central Research Institute for Physics of the Hungarian Academy of Sciences, H-1525 Budapest 114, Hungary[‡]
12 Harvard University, Cambridge, MA 02139, USA
13 Massachusetts Institute of Technology, Cambridge, MA 02139, USA
14 INFN Sezione di Firenze and University of Florence, I-50125 Florence, Italy
15 European Laboratory for Particle Physics, CERN, CH-1211 Geneva 23, Switzerland
16 World Laboratory, FBLJA Project, CH-1211 Geneva 23, Switzerland
17 University of Geneva, CH-1211 Geneva 4, Switzerland
18 Chinese University of Science and Technology, USTC, Hefei, Anhui 230 029, China
19 University of Lausanne, CH-1015 Lausanne, Switzerland
20 Lawrence Livermore National Laboratory, Livermore, CA 94550, USA
21 Los Alamos National Laboratory, Los Alamos, NM 87544, USA
22 Institut de Physique Nucléaire de Lyon, IN2P3-CNRS,Université Claude Bernard, F-69622 Villeurbanne Cedex, France
23 Centro de Investigaciones Energeticas, Medioambientales y Tecnologicas, CIEMAT, E-28040 Madrid, Spain
24 INFN-Sezione di Milano, I-20133 Milan, Italy
25 Institute of Theoretical and Experimental Physics, ITEP, Moscow, Russia
26 INFN-Sezione di Napoli and University of Naples, I-80125 Naples, Italy
27 Department of Natural Sciences, University of Cyprus, Nicosia, Cyprus
28 University of Nymegen and NIKHEF, NL-6525 ED Nymegen, The Netherlands
29 Oak Ridge National Laboratory, Oak Ridge, TN 37831, USA
30 California Institute of Technology, Pasadena, CA 91125, USA
31 INFN-Sezione di Perugia and Universitá Degli Studi di Perugia, I-06100 Perugia, Italy
32 Carnegie Mellon University, Pittsburgh, PA 15213, USA
33 Princeton University, Princeton, NJ 08544, USA
34 INFN-Sezione di Roma and University of Rome, "La Sapienza", I-00185 Rome, Italy
35 Nuclear Physics Institute, St. Petersburg, Russia
36 University of California, San Diego, CA 92182, USA
37 Dept. de Fisica de Particulas Elementales, Univ. de Santiago, E-15706 Santiago de Compostela, Spain
38 Shanghai Institute of Ceramics, SIC, Shanghai, China
39 Bulgarian Academy of Sciences, Institute of Mechatronics, BU-1113 Sofia, Bulgaria
40 Center for High Energy Physics, Korea Advanced Inst. of Sciences and Technology, 305-701 Taejon, Republic of Korea
41 University of Alabama, Tuscaloosa, AL 35486, USA
42 Purdue University, West Lafayette, IN 47907, USA
43 Paul Scherrer Institut, PSI, CH-5232 Villigen, Switzerland
44 DESY-Institut für Hochenergiephysik, O-1615 Zeuthen, FRG
45 Eidgenössische Technische Hochschule, ETH Zürich, CH-8093 Zürich, Switzerland
46 University of Hamburg, W-2000 Hamburg, FRG
47 High Energy Physics Group, Taiwan, China
§ Supported by the German Bundesministerium für Forschung und Technologie
‡ Supported by the Hungarian OTKA fund under contract number 2970.
† Deceased.

References

[1] E. Laermann, T. F. Walsh, I. Schmitt and P. M. Zerwas, Nucl. Phys. B 207 (1982) 205; P. Mättig and W. Zeuner, Z. Phys. C 52 (1991) 37.

[2] ALEPH Collab., D. Decamp et al., Phys. Lett. B 264 (1991) 476.

[3] DELPHI Collab., P. Abreu et al., Z. Phys. C 53 (1992) 555.

[4] L3 Collab., O. Adriani et al., Phys. Lett. B 292 (1992) 472.

[5] OPAL Collab., M. Z. Akrawy et al., Phys. Lett. B 246 (1990) 285;
OPAL Collab., G. Alexander et al., Phys. Lett. B 264 (1991) 219;
OPAL Collab., P. D. Acton et al., Z. Phys. C 54 (1992) 193.

[6] ALEPH Collab., D. Decamp et al., Z. Phys. C 53 (1992) 1.

[7] DELPHI Collab., P. Abreu et al., Nucl. Phys. B 367 (1991) 511.

[8] L3 Collab., B. Adeva et al., Z. Phys. C 51 (1991) 179.

[9] OPAL Collab., G. Alexander et al., Z. Phys. C 52 (1991) 175.

[10] The LEP Collaborations: ALEPH, DELPHI, L3 and OPAL, Phys. Lett. B 276 (1992) 247.

[11] G. Kramer and B. Lampe, Phys. Lett. B 269 (1991) 401.

[12] Z. Kunszt and Z. Trócsányi, ETH Preprint, ETH-TH/92–26.

[13] E. W. N. Glover and W. J. Stirling, Phys. Lett. B 295 (1992) 128.

[14] D. Kirkby, Caltech Preprint CALT-68–1822.

[15] L3 Collab., B. Adeva et al., Nucl. Inst. Meth. A 289 (1990) 35.

[16] JADE Collab., W. Bartel et al., Z. Phys. C 33 (1986) 23;
JADE Collab., S. Bethke et al., Phys. Lett. B 213 (1988) 235.

[17] M. Consoli and W. Hollik, in: Z Physics at LEP 1, CERN Report CERN-89-08, Vol. I, p. 7.

[18] Z. Kunszt and P. Nason, in: Z Physics at LEP 1, CERN Report CERN-89-08, Vol. I, p. 373.

[19] T. Kinoshita, Journ. Math. Phys. 3 (1962) 650;
T. D. Lee and M. Nauenberg, Phys. Rev. 113 (1964) 1549.

[20] G. Kramer and H. Spiesberger, in: Proc. Workshop on Photon Radiation from Quarks (Annecy, December 1991), ed. S. Cartwright (CERN Report CERN-92-04, 1992) p. 26.

[21] F. James and M. Roos, CERN Program Library Document D506 MINUIT (1989).

[22] T. Sjöstrand, Computer Physics Commun. 39 (1986) 347;
T. Sjöstrand and M. Bengtsson, Computer Physics Commun. 43 (1987) 367.

[23] L3 Collab., B. Adeva et al., Z. Phys. C 55 (1992) 39.

[24] G. Marchesini *et al.*, Computer Physics Commun. 67 (1992) 465.

[25] L3 Collab., B. Adeva et al., Phys. Lett. B 248 (1990) 464.

[26] L3 Collab., O. Adriani et al., Phys. Lett. B 284 (1992) 471.

Figure Captions

Fig. 1 Distributions of (a) the final state photon energy, (b) the angle between photons and the nearest jet, and (c) the transverse energy of photons with respect to the event thrust axis. Data points are corrected for detector effects and background from initial state radiation and neutral hadron decays. The predictions of the matrix-element (M. E.) calculation with $\theta_{q\gamma} = 10^\circ$ and 20° are shown as dashed and solid histograms respectively, with fitted values of $\mathcal{N}$ and $\alpha_s^{(1)}$, as given in table 1.

Fig. 2 Linear constraints on the quark electroweak couplings derived from the total hadronic decay width of the Z (thin band), and from theoretical fits to three direct photon distributions (thick band). The Standard Model values of the couplings are shown as a solid circle.

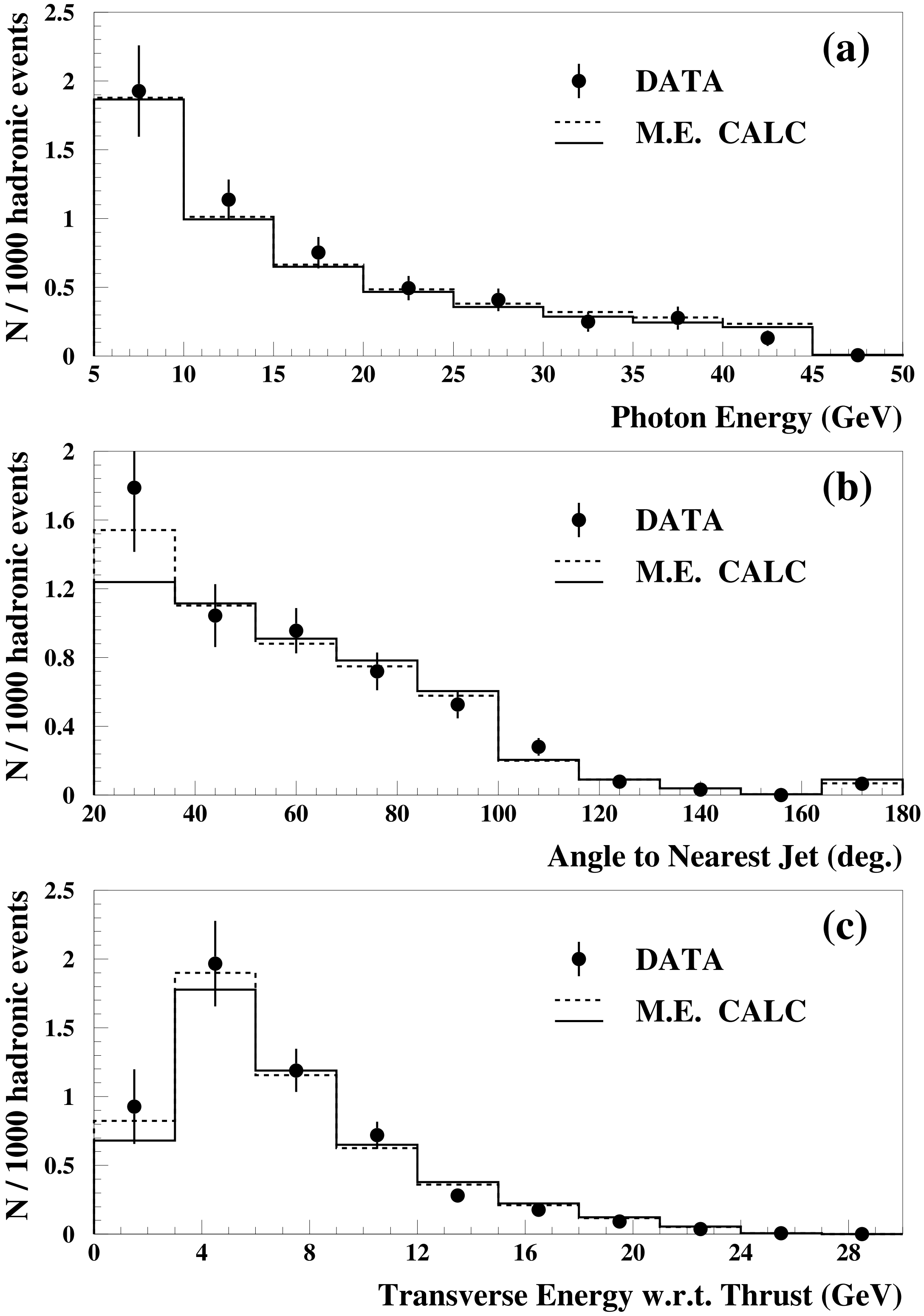
(a)
DATA
M.E. CALC
N / 1000 hadronic events
Photon Energy (GeV)
(b)
DATA
M.E. CALC
N / 1000 hadronic events
Angle to Nearest Jet (deg.)
(c)
DATA
M.E. CALC
N / 1000 hadronic events
Transverse Energy w.r.t. Thrust (GeV)

Figure 1:

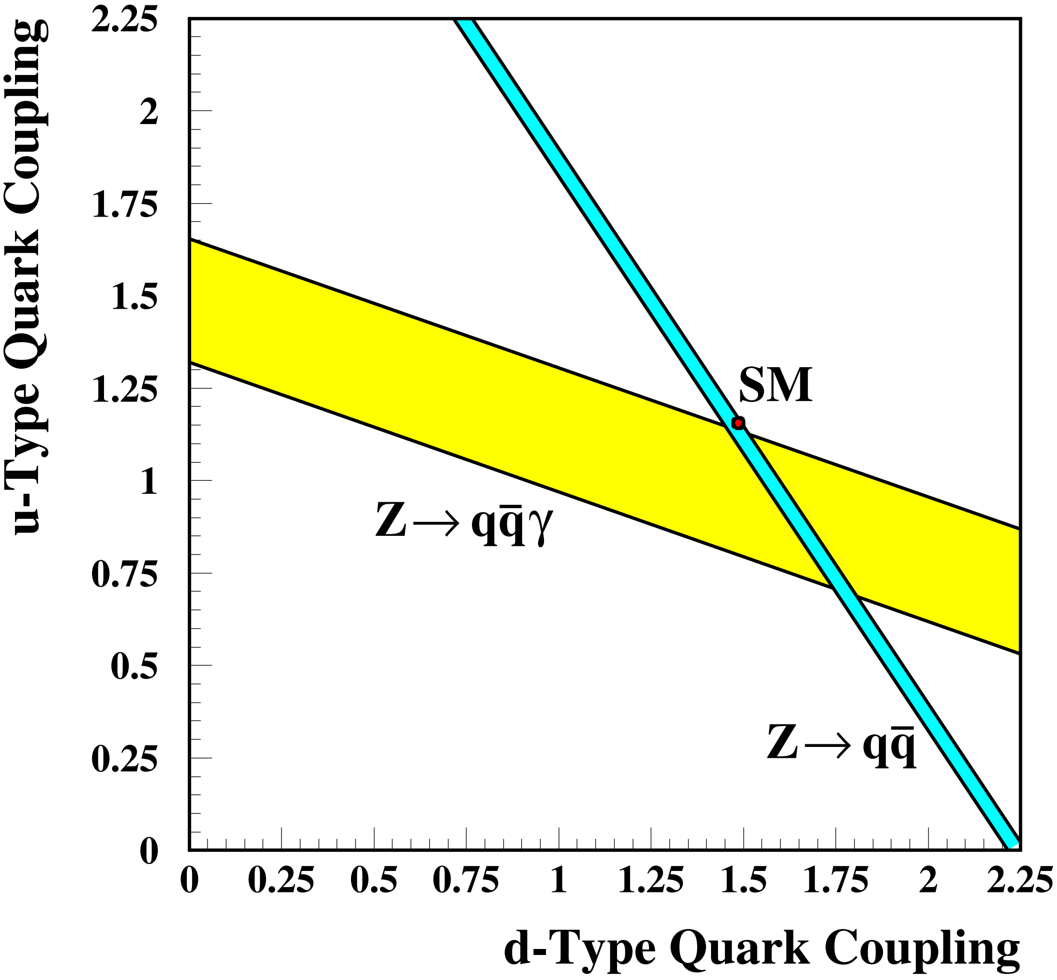
2.25
2
1.75
1.5
1.25
1
0.75
0.5
0.25
0
0
0.25
0.5
0.75
1
1.25
1.5
1.75
2
2.25
u-Type Quark Coupling
d-Type Quark Coupling
SM
Z→ q$\bar{q}$γ
Z→ q$\bar{q}$

Figure 2: